

## Supplementary information

### Phosphonate Functionalized Carbon Spheres as Brønsted Acid Catalysts for Valorization of bio-renewable $\alpha$ -Pinene Oxide to *trans*-Carveol

Amravati S. Singh <sup>a,b</sup>, Jacky H. Advani <sup>a,b</sup>, and Ankush V. Biradar <sup>a,b,\*</sup>

<sup>a</sup>Inorganic Materials and Catalysis Division, CSIR-Central Salt and Marine Chemicals Research Institute (CSIR-CSMCRI), G. B. Marg, Bhavnagar-364002, Gujarat, India

<sup>b</sup>Academy of Scientific and Innovative Research (AcSIR), Ghaziabad 201002, Uttar Pradesh, India

\*Corresponding author: Tel.: +91 278 2567760 Ext: 7170; Fax: +91 278 2566970

Email: [ankush@csmcri.res.in](mailto:ankush@csmcri.res.in)

This SI contains 10 pages, 1 table, 18 Figures

Contents	Page No.
S1. Material Characterizations	2
S2. Scanning electron microscopy (SEM)	3-4
S3. Solid <sup>13</sup> C and <sup>31</sup> P CP MAS NMR spectrum of CS( $\alpha$ ) and PCS( $\gamma$ )	5
S4. XPS survey spectrum of PCS( $\alpha_2$ )	5
S5. Acidic strength calculations of PCS ( $\alpha_2$ ) determine by ICP- OES	5-6
S6. Effect of PCS( $\alpha_2$ ) amount on the distribution of the products in the isomerization of $\alpha$ - pinene oxide	6
S7. Recyclability of the catalyst PCS( $\alpha_2$ )	6
S8. The activity of the catalyst after Hot filtration test	7
S9. SEM and EDAX images of recycled PCS ( $\alpha_2$ )	7
S10. <sup>1</sup> H and <sup>13</sup> C NMR analysis of <i>trans</i> -Carveol	7
S11. Fourier transform infrared spectroscopy (FT-IR) of <i>trans</i> -Carveol	8
S12. GC-MS profile of the products obtained in the isomerization of $\alpha$ -pinene oxide	9-10

## S1. Materials characterizations

The structural characterization studies of the catalyst were carried out by different physiochemical methods. The PXRD analysis was carried out using Philips X'pert MPD system for powder X-ray Diffractometer. The black powder obtained was scanned in the range of 10-80° using Cu K $\alpha$  radiation of 1.54056 Å wavelength with a Ni filter. A Perkin-Elmer GX spectrophotometer was used for the Fourier-transform infrared spectrophotometry (FTIR) spectra using KBr pellets in the wavelength range of 400-4000 cm<sup>-1</sup>. The energy dispersive X-ray (EDX) mapping and morphology of the catalyst was determined using a JEOL JSM 7100F field emission scanning electron microscope (FE-SEM). The synthesized catalyst was dispersed in isopropyl alcohol by sonication and was drop casted on a brass stub. The stub was dried under vacuum and used for analysis. Transmission electron microscope (TEM) (JEOL JEM 2100) was used to analyze the size and shape of the particles and recording the selected area electron diffraction (SAED) of the sample. The samples were loaded on the TEM grid by dispersing it in isopropyl alcohol using ultrasonicator and then drop-casting the suspension on the TEM grid. This drop casted grid was dried in a vacuum oven before analysis. X-ray photoelectron spectroscopy (XPS) was performed using an ESCA+ (Omicron Nanotechnology, Germany) with a monochromatized Al-K $\alpha$  X-ray ( $h\nu = 1486.7$  eV) as the excitation source (15 kV and 20 mA). The pass energy for the survey spectrum was 50 eV and 20 eV in case of the short scan. The sample was placed on the copper tape and degassed in the XPS FEL chamber to minimize the air contamination. A charge neutralizer of 2 keV was used to overcome any charging problem, and the calibration was done using the adventitious C 1s feature at 284.6 eV as a reference. All the spectra's were recorded at 90° of the X-ray source. <sup>31</sup>P and <sup>13</sup>C solid-state nuclear resonance (NMR) spectroscopy was performed using a Bruker 11.7 T spectrometer equipped with a triple resonance 2.5 mm solid-state probe head and an avance III console. Samples were prepared for NMR by ultrasonic ion in acetone for 5 min, then dried at 80°C, and filled into a 2.5 mm zirconia rotor. All experiments were performed at room temperature, either in static mode or while spinning the sample at 20kHz magic angle spinning (MAS) frequency. The <sup>31</sup>P chemical shift was determined with reference to 85% H<sub>3</sub>PO<sub>4</sub> in D<sub>2</sub>O and the <sup>13</sup>C chemical shift was determined with reference to Si(CH<sub>3</sub>)<sub>4</sub>. The number of transients recorded was 2000 for <sup>31</sup>P NMR experiments, and 16000-24000 for <sup>13</sup>C NMR experiments. The classical Hahn echo pulse sequence was used for <sup>31</sup>P NMR experiments, and a simple 30°-one pulse excitation sequence was used for all <sup>13</sup>C NMR and <sup>31</sup>P NMR experiments (as indicated). All spectra were acquired without decoupling. The recycle delay was set to 2s, the

echo delay to 0.2 ms, and the pulse length for 90° flip angle experiments to 5  $\mu$ s for  $^{31}\text{P}$  NMR experiments. The thermogravimetric analysis (TGA) was carried out on a Mettler TGA/DTA 851e instrument at a nitrogen flow rate of 50 mL/min. The surface area of the catalyst was obtained using the ASAP 2010, Micromeritics Sorptometer at 7.4 K. The sample was degassed at 150  $^{\circ}\text{C}$  for 10h prior to sorption. ICP- OES analysis done by Perkin Elmer, optima, 2000 instrument.

## S2. Scanning electron microscopy (SEM)

### S2.1. SEM images of CS( $\alpha$ )

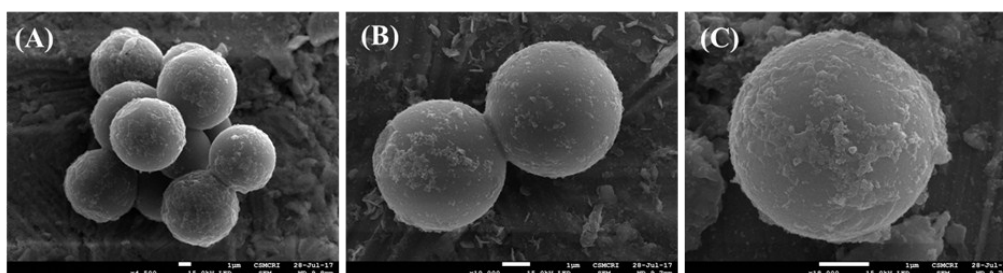


**Fig. S1.** Scanning electron microscopy (SEM) image of CS( $\alpha$ ) (A-C).

### S2.2. SEM images of PCS( $\alpha_1$ )

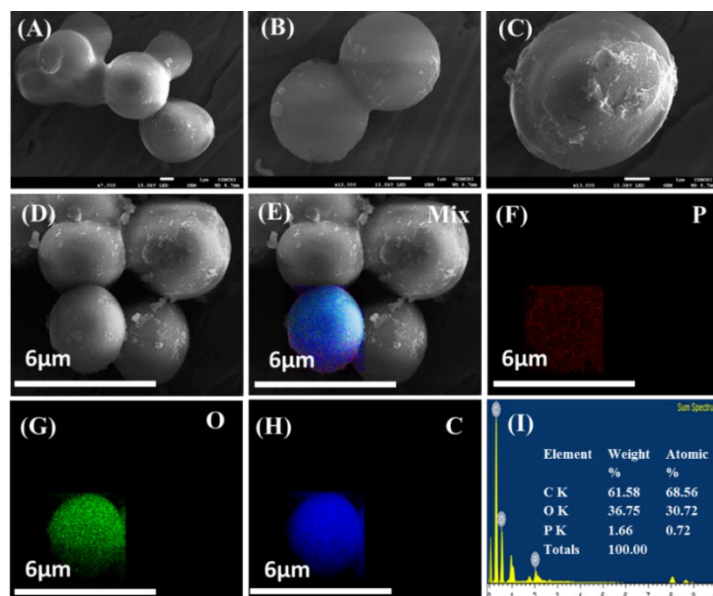


**Fig. S2:** SEM images of PCS( $\alpha_1$ ) (A-D) and SEM elemental mapping of PCS( $\alpha_1$ ) where E shows overall mapping, F- shows phosphorous, G-shows oxygen and H-shows carbon. And I shows the SEM-EDAX of the sample. And Table shows the % availability of the elements.

### S2.3. SEM and EDAX images of CS( $\gamma$ )

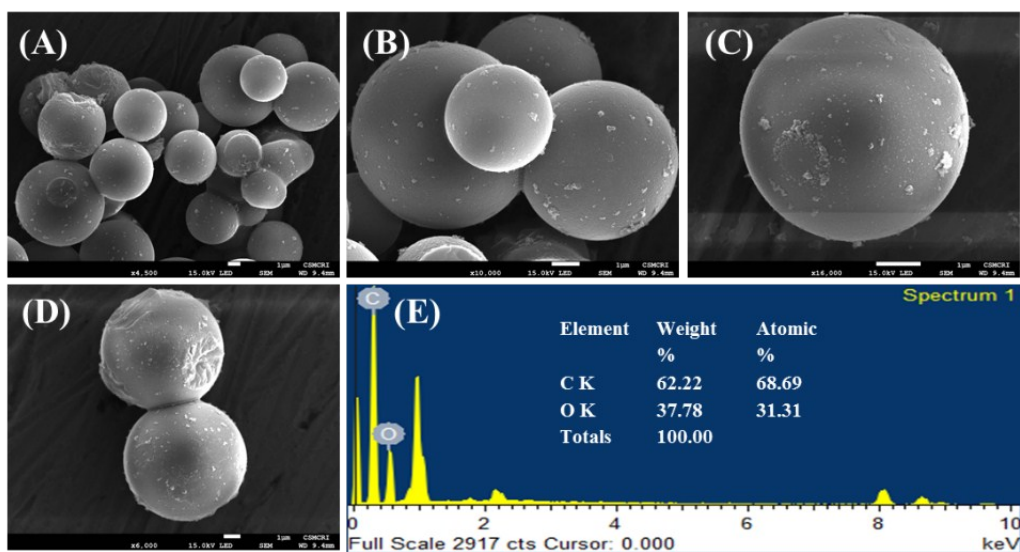


**Fig. S3.** Scanning electron microscopy image of CS( $\gamma$ ) (A-D) and E show the SEM-EDAX of the sample and Table shows the the % availability of the elements.

### S2.4. SEM images of PCS( $\gamma$ )

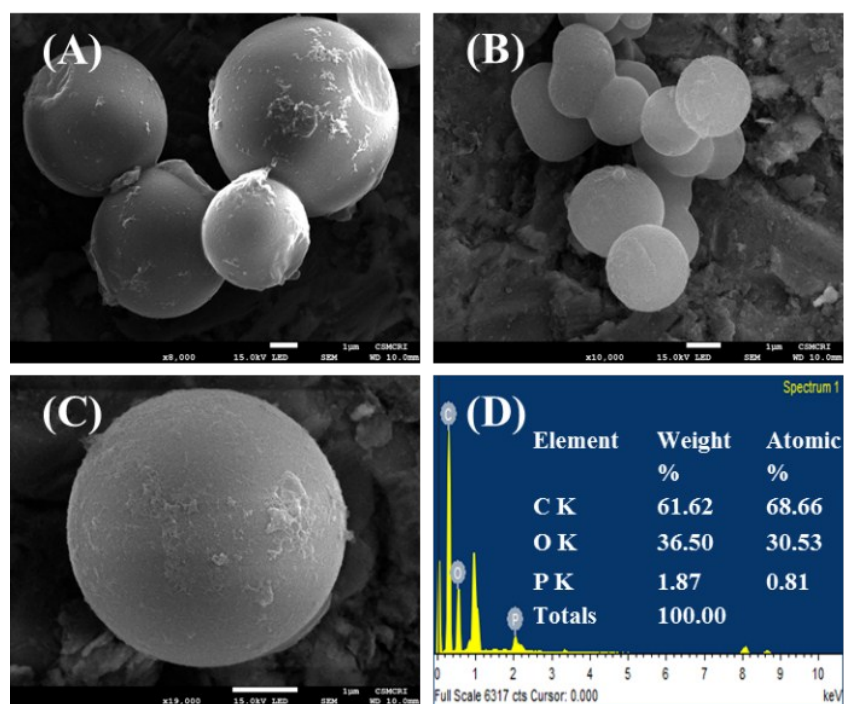


**Fig. S4:** Scanning electron microscopy (SEM) image of PCS( $\gamma$ ) (A-C) and D show the SEM-EDAX of the sample. And Table shows the % availability of the elements.

### S3. Solid $^{31}\text{P}$ and $^{13}\text{C}$ NMR of CS ( $\gamma$ ) and PCS ( $\gamma$ )

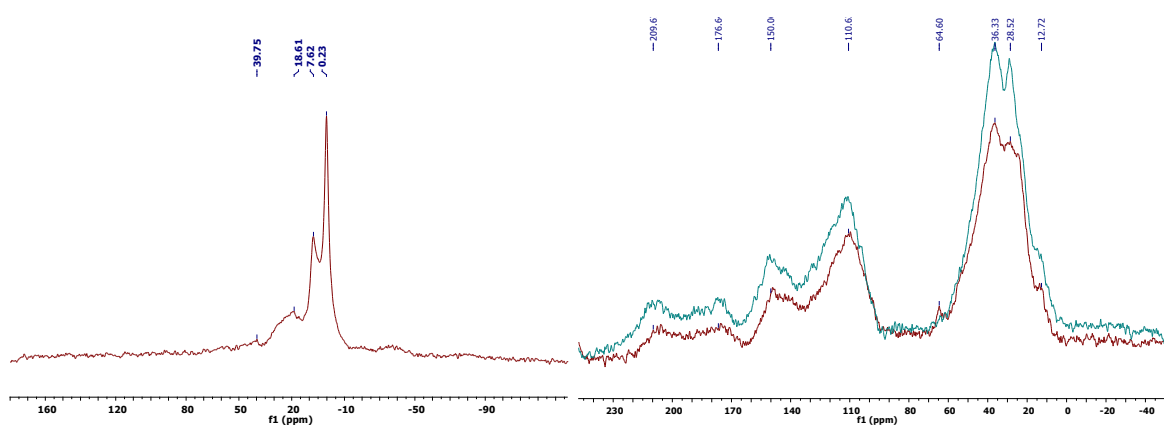


**Fig. S5. (a)** Solid-state  $^{31}\text{P}$  NMR of PCS ( $\gamma$ ) **(b)** Comparison solid  $^{13}\text{C}$  NMR of CS ( $\gamma$ ) and PCS ( $\gamma$ ).

### S4: XPS survey spectrum of PCS ( $\alpha_2$ )

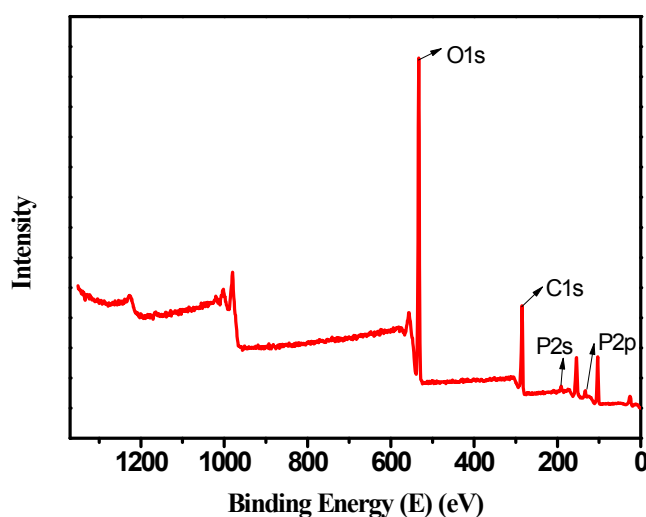


**Fig. S6.** X-ray photoelectron spectroscopy (XPS) survey spectrum of PCS( $\alpha_2$ ).

### S5: Acidic strength calculations of PCS ( $\alpha_2$ ) determine by ICP- OES

The 100 mg of PCS( $\alpha_2$ ) catalyst was digested Aqua regia solution and analyzed by ICP-OES.

The P content was found 1.33 wt%

Mole of P was calculated as follows:

100 mg = 1.33 wt% of phosphorus

=1.33 mg phosphorus in 100 mg PCS( $\alpha_2$ )

=13.3 mg phosphorus in 1000 mg PCS( $\alpha_2$ )

13.3 mg = 0.0133g phosphorus

Moles of phosphorus = Weight/Mol. Wt (MW of P-30.97)

$$= 0.0133/30.97$$

$$= 0.00042 \text{ moles/g}$$

$$= 0.42 \text{ mmoles/g of phosphorus}$$

**S6. Table S1.** Effect of PCS( $\alpha_2$ ) amount on the distribution of the products in the isomerisation of  $\alpha$ - pinene oxide.

Entry	Weight (mg)	Conv. (%)	Selectivity (%)			
			TCV	CPA	TPC	Others
1.	10	71	66	20	7	7
2.	20	80	66	21	7	6
3.	30	88	67	19	6	8
4.	40	94	67	20	7	6

**Reaction condition:**  $\alpha$ - pinene oxide: 0.5 g (3.28 mmol); Catalyst: PCS ( $\alpha_2$ ): Solvent: DMF (2 mL); Temp. : 140 °C; Time: 1 h.

**S7. Recyclability of the catalyst PCS( $\alpha_2$ )**

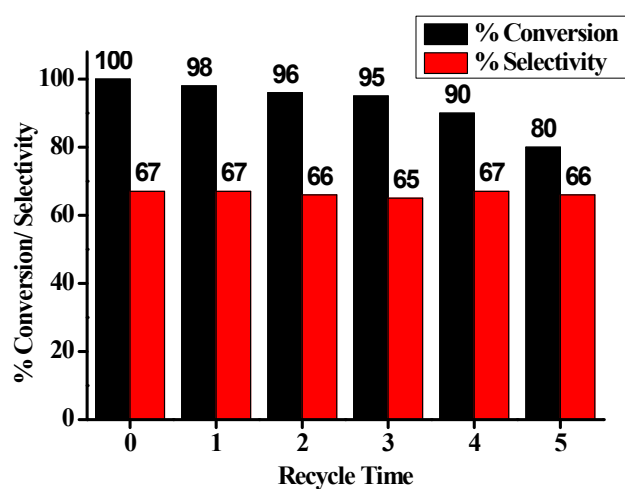


**Fig. S7.** Recyclability of PCS( $\alpha_2$ ) catalyst.

### S8. Activity of the catalyst after Hot filtration test

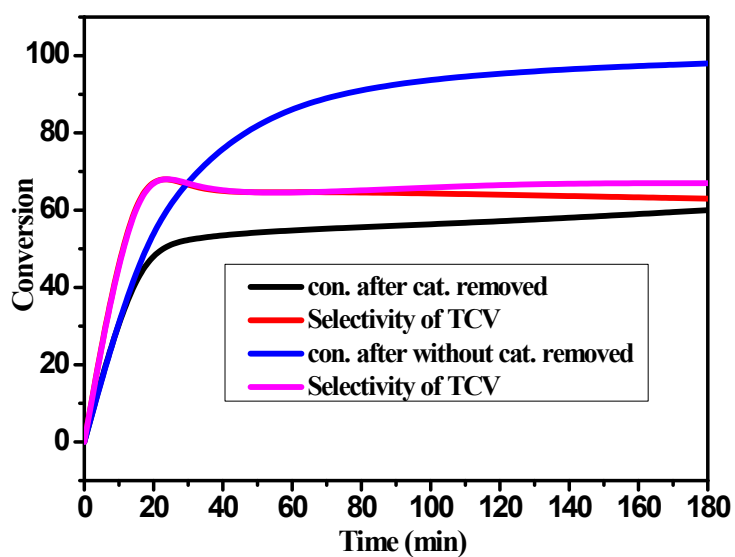


Fig. S8. Activity of the catalyst after Hot filtration test.

### S9: SEM and EDAX images of recycled PCS ( $\alpha_2$ )

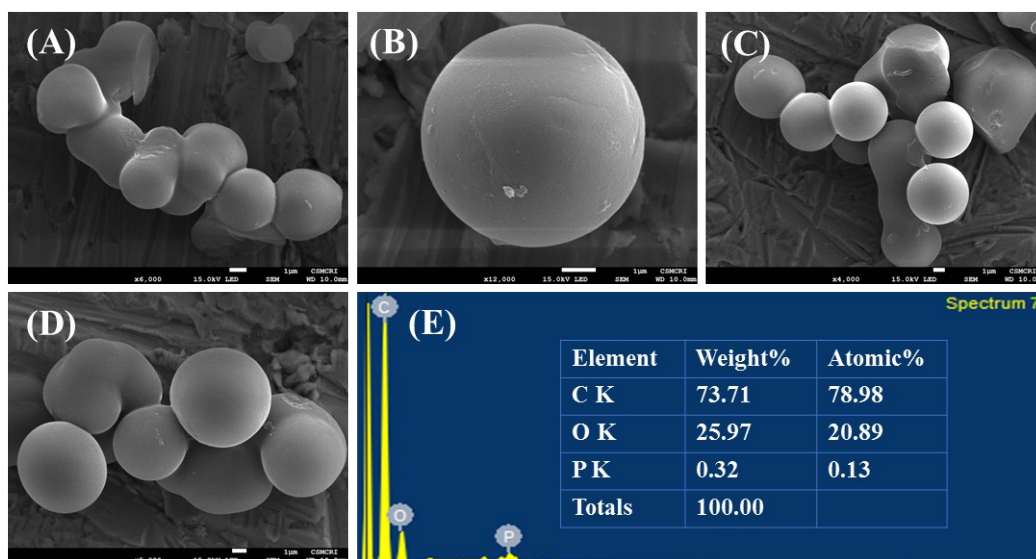


Fig. S9. Scanning electron microscopy (SEM) image of recycled PCS( $\alpha_2$ ) (A-D) and E show the SEM-EDAX of the sample. And Table shows the % availability of the elements.

### S10. $^1\text{H}$ and $^{13}\text{C}$ NMR analysis of *trans*-Carveol

$^1\text{H}$  NMR of *trans*-Carveol  $\text{CDCl}_3$  (600 MHz)  $\delta$  5.59 (s, 1H), 4.75 (s, 2H), 4.02 (s, 1H), 2.34 (s, 1H), 2.13 (s, 1H), 1.93 (s, 1H), 1.85 (s, 1H), 1.80 (s, 3H), 1.75 (s, 3H), 1.61 (s, 2H)

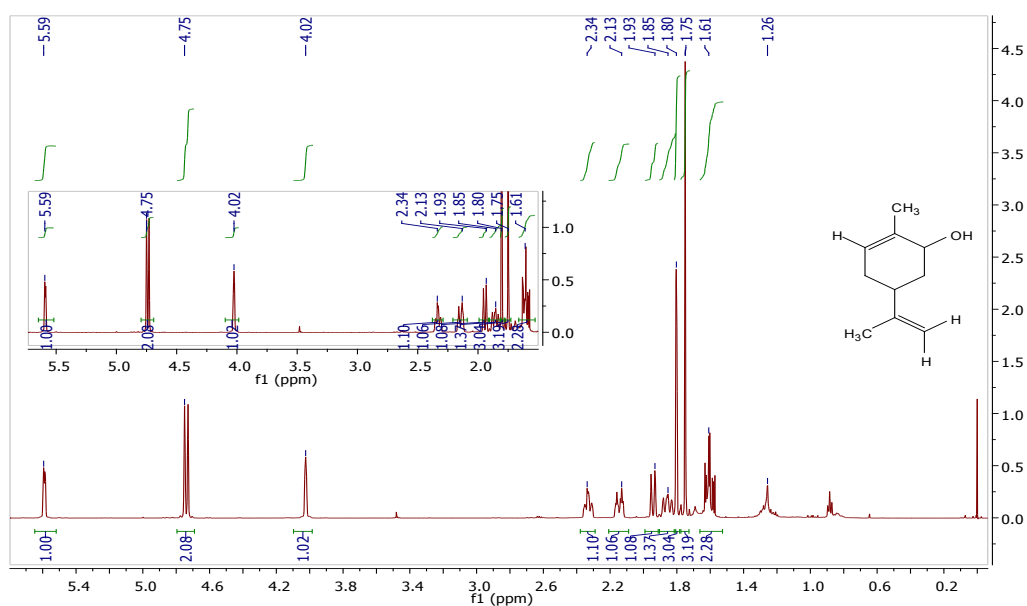


Fig. S10.  $^1\text{H}$  NMR of *trans*-Carveol

$^{13}\text{C}$  NMR of *trans*-Carveol  $\text{CDCl}_3$  (600 MHz)  $\delta$  148.17 (s), 133.29 (s), 124.35 (s), 108.01 (s), 67.52 (s), 35.71 (s), 34.20 (s), 29.98 (s), 28.69 (s), 19.85 (s).

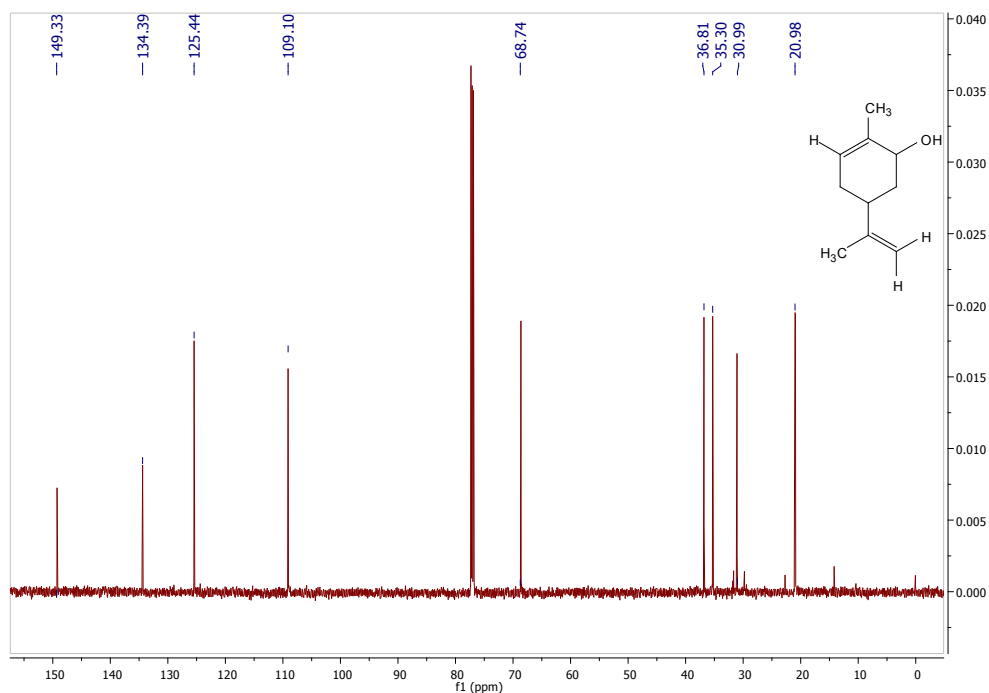


Fig. S11.  $^{13}\text{C}$  NMR of *trans*-Carveol.



S11. FTIR spectrum of *trans*-Carveol.

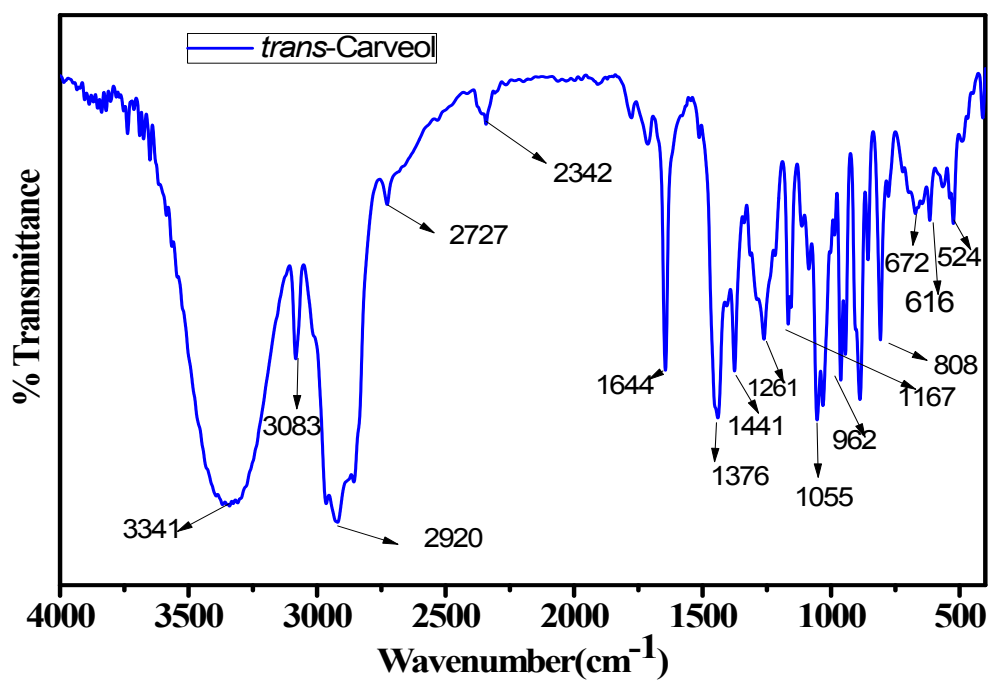


Fig. S12. Fourier transform infrared spectrum of *trans*-Carveol.

S12. GC-MS profile of the selected products.

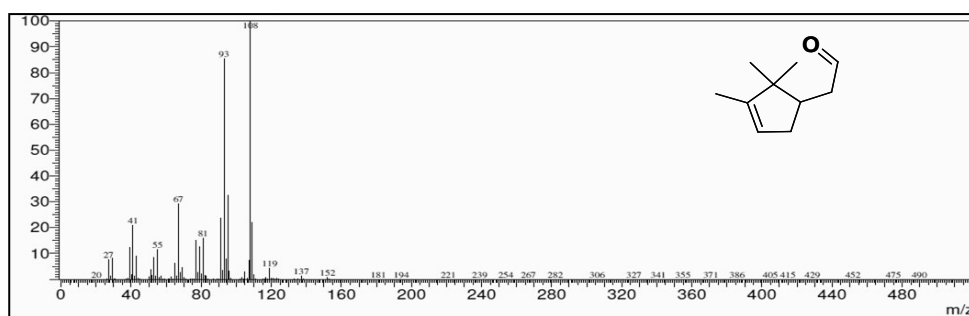


Fig. S13. GC-MS profile for Campholenic aldehyde.

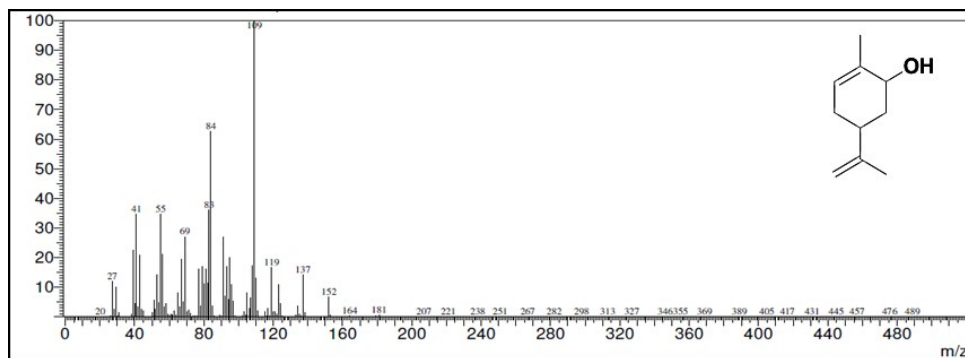
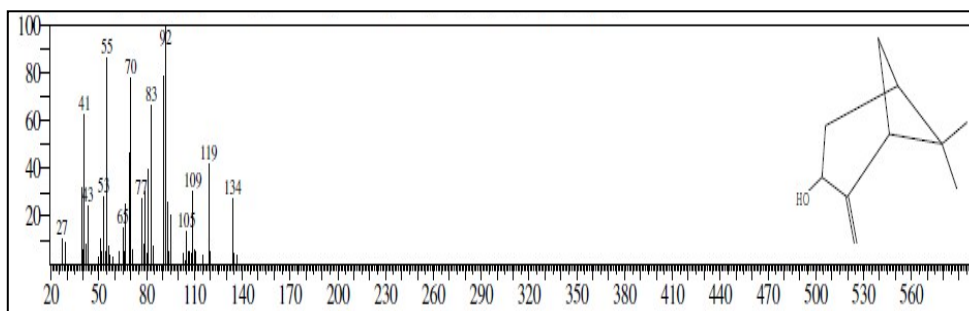
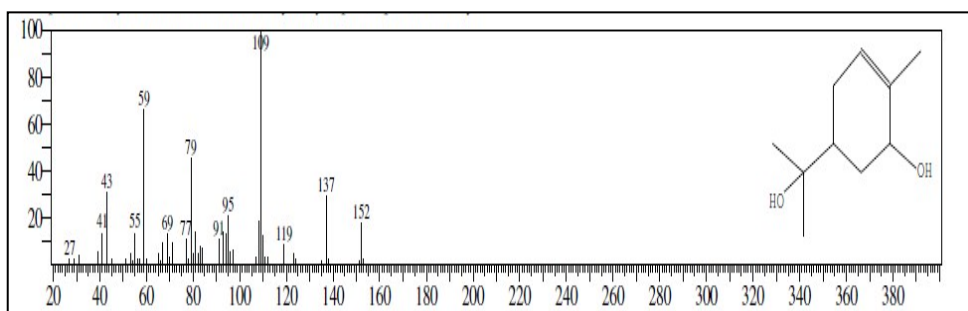


Fig. S14. GC-MS profile for *trans*-Carveol.



**Fig. S15.** GC-MS profile for *trans*-pinocarveol.



**Fig. S16.** GC-MS profile for *trans*-Sobrerol.

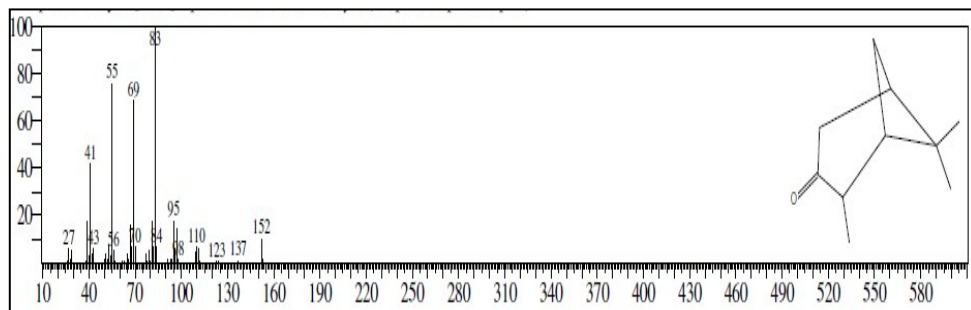


**Fig. S17.** GC-MS profile for *trans*-Pinocarvone.

\*\*\*\*\*